NASA TECHNICAL MEMORANDUM

NASA TM X-73635

NASA TM X-73635

VELOCITY AND TEMPERATURE PROFILES IN NEAR-CRITICAL NITROGEN FLOWING PAST A HORIZONTAL FLAT PLATE

by Robert J. Simoneau
Lewis Research Center
Cleveland, Ohio 44135

ABSTRACT

Boundary layer velocity and temperature profiles were measured for nitrogen near its thermodynamic critical point flowing past a horizontal flat plate. The heated surface was oriented both facing upward and downward. The results were compared to earlier work in which measurements were made for vertically upward flow. The boundary layer temperatures ranged from below to above the thermodynamic critical temperature. For wall temperatures below the thermodynamic critical temperature there was little variation between the velocity and temperature profiles in the three orientations. In all three orientations the point of crossing into the critical temperature region is marked by a significant flattening of the velocity and temperature profiles and also a decrease in heat transfer coefficient. As the heat flux and, consequently, wall temperature are further increased significant changes occur in the velocity and temperature profiles. Examination of near-critical heat transfer in these three flow orientations offers insights into the relative role of buoyancy forces in this regime.

NOMENCLATURE

C_p	specific heat capacity, J/g K
g	acceleration of gravity, cm/sec^2
Gr_x	Grashof number, $\rho_\infty(\rho_\infty - \rho_w)x^3 g/\eta_\infty^2$
h	heat transfer coefficient, W/cm^2 K
Nu_x	Nusselt number, hx/λ
P	pressure, MPa
Pr	Prandtl number, $\eta C_p/\lambda$
q	heat flux, W/cm^2
Re_x	Reynolds number, $\rho_\infty u_\infty x/\eta_\infty$
St_x	Stanton number, $h/U_\infty \rho_\infty C_{p_\infty}$
T	temperature, K
U	velocity, m/sec
x	distance from leading edge of plate, cm
y	normal distance from the plate, mm
λ	thermal conductivity, W/cm K
η	dynamic viscosity, g/cm-sec
ρ	density, g/cm^3

Subscripts

c	critical point conditions
calc	calculated
exp	experimental
w	wall conditions
x	conditions at axial position x along the plate
∞	free stream conditions

INTRODUCTION

Because of low research activity, designers are reluctant to work with fluids near their thermodynamic critical point; however they remain of interest in design. The space industry stores its cryogenic liquids above their critical pressure to avoid having vapor present in a low gravity field. Supercritical power cycles have some attractive features and the cooling of cryogenic equipment, such as cryomagnets, is a continuing need. Much of the low confidence for design analyses stems from a lack of detailed knowledge of the mechanisms at work, especially in forced convection. Surveys by Hendricks, et al. (1), Hall (2), and Petukhov (3) yield a fairly comprehensive picture of the status of near-critical heat transfer. Experiments probing the details of forced convection in near-critical fluids have been limited. An early paper by Wood and Smith (4) revealed the M-shaped velocity profile which obtained its maximum between the wall and tube centerline. Sabersky and Hauptmann (5) added some detail on flow over a flat plate, including some fine photographs. Three papers at the 1971 National Heat Transfer Conference (6-8) presented velocity and temperature profile measurements in various configurations. One of them, Simoneau, et al. (6), examined vertically upward flow past a heated flat plate. The authors claimed the results indicated the presence of a strong body force effect. The present paper extends that work to horizontal flow.

It was the purpose of the experiment being reported herein to examine further the conclusion on the influence of buoyancy by comparing detailed measurements taken in both horizontal and vertical flow. Thus, a set of conditions from reference 6, which yielded a wide range of effects, was selected to be repeated in horizontal flow. The nominal conditions for this comparison were: $P_\infty = 3.74$ MPa ($P_\infty/P_c = 1.10$); $T_\infty = 110.3$ K ($T_\infty/T_c = 0.874$); and $Re_{x,\infty} = 1.03 \times 10^6$. Data were taken at these conditions in

1

horizontal flow with the heated surface both facing
upward and facing downward. These horizontal flow
data are compared with the vertical flow data.

Note should be made of a discrepancy that exists
between this and the earlier work (6). A newer
thermophysical property program, GASP (9), is used
herein. It has an updated viscosity equation which
changes the Reynolds number calculation. Reynolds
numbers herein are about 10 to 13 percent higher.
Any earlier data used herein has the Reynolds number
recomputed using the newer program, GASP (9).

EXPERIMENTAL APPARATUS

The basic flow rig is shown in figure 1. It was
a once-through or blow-down type system. Liquid ni-
trogen was transferred from a low pressure supply to
the 0.4 m³ high pressure dewar. The fluid tempera-
ture was controlled by bubbling nitrogen gas through
the dewar. Nitrogen gas, at the desired pressure,
was applied to the top of the fluid to force the
fluid through the system. System pressure and flow
rate were maintained by the use of throttling valves.
The system was heavily insulated and was precooled
from an auxiliary supply. The system was designed so
that the test section could be placed either in the
horizontal or vertical position.

The test section details are shown in figure 2.
The test section was of rectangular cross-section of
about 6 to 5 aspect ratio. It contained two 2.5 cm
wide by 15 cm long Nichrome plates back to back, in-
sulated from each other by a bakelite centerbody.
The first centimeter was a copper electrode and was
unheated. The primary surface was instrumented
longitudinally with 11 Chromel-Constantan thermo-
couples electrically isolated from the heater. The
opposite surface served as a guard heater and was
also instrumented. Heat was generated by the dissi-
pation of direct-current power.

The boundary layer surveys were made with a com-
bination pitot-static and thermocouple probe (fig. 3)
which was traversed through the boundary layer toward
the primary heater surface. The distance from the
primary heater surface to the opposite wall was about
2.4 cm, which was approximately 10 times the boundary
layer thickness. On the back side the distance to
the wall was 0.72 cm, about three times the boundary
layer thickness. The temperature portion of the
probe was an exposed ball, Chromel-Constantan thermo-
couple encased in a sheath with an overall diameter
of 0.25 mm. The dynamic pressure part of the probe
was a two leg pitot-static probe of rectangular
cross-section at the tip and had an overall tip
height of 0.25 mm. The total pressure leg had a
0.13 by 0.70 mm opening at the tip. The static port
was a 0.38 mm diameter hole located six thicknesses
from the tip to avoid separation. Measurements could
be made to within 0.14 mm of the wall. All of the
surveys reported herein were made 13.1 cm from the
leading edge of the plate.

An important feature of this design was making
both legs of the probe identical. This was done in
order to match the response lags in the lines, re-
ducing the noise, and also to assure the same density
gradient in each leg to avoid static head errors.
The probe noise that did appear was assessed to be
due to very small static pressure perturbations.

Flow rates were measured with venturi flow meters.
All system pressures were measured with strain gage
transducers, except at the probing station where the
system static pressure was measured with a high pre-
cision balance type transducer accurate to ±0.05 per-
cent. The dynamic head was measured with a variable
reluctance type transducer. System temperatures were
measured with platinum resistance thermometers. The
heater plate thermocouples were standard Chromel-
Constantan. All signals, including test section volt-
age and current, were sensed with a precision digital
voltmeter and recorded on a digital data acquisition
system. All measurements were checked by some kind of
redundant instrument.

The system was brought up to nominal operating
conditions and allowed to stabilize on some near-
nominal operating condition. At this point a traverse
of the probe from the free stream to the plate was be-
gun. The traverse was made by moving the probe in
about 15 discrete steps, stopping at each step to ac-
quire data. Because of the probe noise mentioned
earlier, at each step the signals were electronically
integrated for about 3 seconds. The integrated sig-
nals and all system parameters were recorded and the
probe was moved to the next position. Because of the
blow down configuration with a fixed supply of liquid
nitrogen, this procedure limited the number of points
per traverse to about 15, which in general was suffi-
cient to describe the profile. In addition the bulk
fluid temperature had a tendency to drift steadily up-
ward about 1 K during a traverse. The free stream
conditions reported are the average over the traverse
time.

RESULTS

For reference let us first examine the velocity
distribution over the unheated plate. Figure 4 shows
a series of velocity profiles for both gas and liquid
flow at zero heat flux in all three geometric orienta-
tions. In both the gas and liquid cases the profiles
appear to be rather conventional and there appears to
be no particular bias according to geometric orienta-
tion. The gas has about a 1/6 power profile, whereas
the liquid is more toward 1/5 power. In both cases,
the edge of the boundary layer is approximately 2.0 mm
from the heater surface. The scatter in the data from
run to run is about 2 percent.

Turning now to the near critical fluid with heat
transfer, a summary of the range of extremes that were
obtained in these experiments is illustrated in the
velocity profiles shown in figure 5. In the vertically
upward flow the velocity profile exhibits a maximum
between the wall and the free stream. On the other
hand, in the horizontal flow with the heater facing
downward the velocity appears to go to zero at the
probe location nearest to the wall. The velocity
profile with the heater facing upward is more normal
looking, however, it too has quite a steep gradient.

With that introduction as a reference, let us
look at a complete set of velocity and temperature
profiles for each of the flow orientations. Figures
6, 7, and 8 are velocity and temperature profiles for
vertically upward flow, horizontal flow with the
heater facing upward, and horizontal flow with the
heater facing downward, respectively. In each case
the nominal operating parameters are: $T_\infty = 110.3$ K,
$P_\infty = 3.744$ MPa, ($T_c = 126.3$ K, $P_c = 3.417$ MPa), $U_\infty =$
0.660 m/sec, and $Re_{x,\infty} = 1.03 \times 10^6$. The surface heat

flux is varied from 3 to 15 watts/cm^2, which in turn causes the wall temperature at the probing station to vary from 23 K (below T_c) to over 200 K (well above T_c). In all cases the bulk of the fluid, the free stream, is below the thermodynamic critical temperature, thus, whenever $T_w > T_c$, the critical temperature occurs somewhere in the boundary layer.

In the vertically upward flow case (fig. 6), the effect of the boundary layer moving into the critical region is most pronounced. At the lowest heat flux (q = 3.1) the wall temperature remains below the thermodynamic critical temperature and the profiles have a rather conventional appearance to them. When the heat flux is raised sufficiently to cause the wall temperature to exceed the critical temperature the velocity profiles begin to show unusual shapes, first getting quite flat and then, as heat flux is increased, exhibiting a maximum between the wall and the free stream. This effect was first observed by Wood (4) in a vertical tube experiment. In that case the presence of two walls produced two maxima and the profile had the shape of an M. The terminology M-shaped profiles is quite descriptive and has been carried in the literature. The corresponding temperature profiles kept getting flatter as heat flux increased, until at the higher heat fluxes the profiles tended to converge on each other. These observations were reported in reference 6 and it was also observed that the significant change in behavior was accompanied by a five-fold increase in Grashof number.

To further examine this without the parallel body force the test section assembly was placed in the horizontal position. Looking, first, at results for the heater surface facing upward, the velocity and temperature profiles e shown in figure 7. The dramatic M-shaped velocity profiles of upward flow are not present. On the other hand, both the velocity and temperature profiles exhibit marked inflection points at about y = 1 mm for the higher heat fluxes. An examination of the temperature profiles reveals no special thermodynamic effect, such as crossing the critical temperature, occurring in this region. In fact, in all of the profiles, for all heat fluxes, the thermodynamic critical temperature occurs very near the wall. It is interesting to note that for q = 9, 12, and 15 watts/cm^2 the fluid temperatures at y = 0.14 mm are almost the same, being 123.5, 124.0, and 125.4 K, respectively, while at the same time the wall temperatures are 173, 210, and 255 K, respectively. The energy required to drive the boundary layer through the critical temperature appears to be quite large. This is consistent with the tendancy of the temperature profiles to get increasingly steep near the wall and then flatten out away from the wall as the heat flux increases. Since buoyancy is normal to the flow, the inflection of the velocity profiles at higher heat fluxes could be interpreted as an acceleration of the fluid near the wall due to thermal expansion. This question was raised concerning the upward flow data when it was first acquired. Were the so-called M-shaped profiles in velocity the result of buoyancy or fluid acceleration? It would appear that, while acceleration forces may influence the vertically upward flow, they are not strong enough to produce the M-shape.

The final set of data, the velocity and temperatures in horizontal flow with the plate facing downward (fig. 8), are also useful in addressing the question of the relative roles of buoyancy and acceleration.

The most striking observation in these velocity profiles is that for two profiles the velocity goes to zero at a probing station a finite distance from the wall. Actually the transducer readings oscillated about zero and, since the values were well within the error level of the transducer, they can only be qualitatively interpreted. While one could question the validity of saying the velocity goes to zero somewhere in the boundary layer, it is clear from the data points at slightly greater values of y that the velocity is dropping off very rapidly in the boundary layer at some finite distance from the wall. The temperature profiles also exhibit curious behavior. At q = 15.3 the fluid temperature sensed by the probe at y = 0.14 was greater than the wall temperature. It appears that a highly unstable condition existed here and that local pockets of stagnant fluid were accumulating near the wall. This unstable condition was observed experimentally in the wall temperatures as well and it was very difficult to operate the facility. In fact, at one point the test plate over-heated to the point of loosening the thermocouples. Although the temperature profiles tend to become flatter as heat flux increases, the barrier near the critical temperature is not as strong in these boundary layers.

A couple of observations can be made by taking together the three sets of profiles which represent the three different flow geometries. First, both fluid acceleration and body forces play a role in shaping the velocity profiles, but body forces appear more dominant. Second, most of what is happening occurs very close to the wall, much closer than in conventional flows. One curious result is that at q = 6 watts/cm^2 all three geometric orientations yield the same wall temperature, 145 to 147 K. Even though the velocity profiles are much different from case-to-case, the temperature distributions are quite similar. It is only above q = 6 watts/cm^2 that wide variations occur in the results produced by the different flow orientations.

Some additional insight can be gained by examining the heat transfer coefficients. These are tabulated along with the system parameters for each run in table I. Table I also includes a calculated heat transfer coefficient. This is based on an equation from Kays (10) for turbulent flow over a flat plate with uniform surface heat flux

$$St_x = 0.0307 \ Re_{x,\infty}^{-0.2} \ Pr_\infty^{-0.4}$$

The choice of heat transfer equation is somewhat arbitrary for this discussion. What is required is an equation which will describe turbulent heat transfer in forced convection over a flat plate and the above is a logical choice for that. Examination of the ambient gas data for horizontal flow in table I suggests that the Kays equation may be about 15 to 16 percent low in the present test application.

The gas heat transfer coefficient for vertical flow listed in table I is about 32 percent above the average for horizontal flow. To examine whether free convection could account for the increased heat transfer a standard textbook equation was selected from Eckert and Drake (11)

$$Nu_x = 0.10 \ (Pr_\infty Gr_{x,\infty})^{1/3}$$

For the conditions of the vertical gas run this equation yields a free convection heat transfer coefficient, 0.00583 watts/cm^2, which is 19 percent of the

3

forced convection value. Thus it seems possible that free convection augmentation could be sufficient to produce to increased heat transfer in vertical gas flow.

In liquid nitrogen at $q = 3$ watts/cm^2, where the wall temperature is below critical, the results are qualitatively similar to the gas. In the liquid, however, the experimental increase in vertical flow is a more modest 11 percent, whereas the computed free convection coefficient is about 40 percent of the computed forced convection value. The important point to note is that in all instances, regardless of geometric orientation, the heat transfer coefficients drop off as the heat flux is increased to values which cause the wall temperature to go above the critical temperature. In almost all instances these values are well below those for heat transfer to sub-critical temperature liquid nitrogen as computed by standard equations such as that of Kays'. Calculations with properties calculated on the basis of wall or film temperatures yield no better results.

Another way of looking at this is to examine the behavior of the Grashof number. In figure 9 the Grashof number is plotted for the nominal operating conditions of the experiment as a function of wall temperature. The Grashof number rises steeply and increases an order of magnitude as the wall passes through the critical temperature region. It was noted in reference 6 that the unusual behavior began in a range $1.6 < Gr_x/Re_x^2 < 3.0$. For the present experiment this would be $1.70 \times 10^{12} < Gr_x < 3.18 \times 10^{12}$. The Grashof plot shows that the body force has increased significantly in the exact range where all the anomalies begin. Of course, the Grashof number, as defined, is only meaningful in the vertical orientation.

SUMMARY AND CONCLUSIONS

An experiment has been conducted in which nitrogen near its thermodynamic critical point was flowed past a heated flat plate. The plate was horizontal and data were taken for both heater facing upward and downward. This was compared with earlier data taken in vertically upward flow. The velocity and temperature profiles taken in these three orientations provide a comprehensive and consistent set of data for analysts to use to develop their theories.

In all geometric orientations the velocity profiles were strongly affected when the wall temperature exceeded the critical temperature. In upward flow a maximum occurred in the velocity between the wall and the free stream. In horizontal flow with the plate facing upward a distinct inflection occurred in the velocity profiles. In horizontal flow with the plate facing downward there were stagnant regions where the velocity went to zero.

It was observed that it was very difficult to get the fluid in the boundary layer to cross the critical temperature. Thus, the temperature gradients were very steep near the wall, much steeper than normal.

Examining the profiles from the three orientations together, it appears that both fluid acceleration due to expansion and due to body force occur. In the orientations where body force can influence the flow it seems to be a much more dominant force.

Heat transfer coefficients drop off sharply as the wall temperature increases above the critical temperature. They are well below what one would compute for turbulent forced convection heat transfer to liquid nitrogen flowing past a flat plate.

The threshold of the region of anomalous behavior associated with near-critical fluids begins when the wall temperature is slightly above the critical temperature. The heat flux which will produce this threshold temperature can be predicted by conventional correlation.

REFERENCES

1 Hendricks, R. C., Simoneau, R. J., and Smith, R. V., "Survey of Heat Transfer to Near Critical Fluids," Advances in Cryogenic Engineering, Vol. 15, K. D. Timmerhaus, ed., Plenum Press, New York, 1970, pp. 197-237.
2 Hall, W. B., "Heat Transfer Near the Critical Point," Advances in Heat Transfer, Vol. 7, T. F. Irvine, Jr. and J. P. Hartnett, eds., Academic Press, New York, 1971, pp. 1-86.
3 Petukhov, B. S., "Heat Transfer in a Single-Phase Medium Under Supercritical Conditions," High Temperature, Vol. 6, 1968, pp. 696-709.
4 Wood, R. D. and Smith, J. M., "Heat Transfer in the Critical Region - Temperature and Velocity Profiles in Turbulent Flow," AIChE Journal, Vol. 10, 1964, pp. 180-186.
5 Sabersky, R. H. and Hauptmann, E. G., "Forced Convection Heat Transfer to Supercritical Pressure Carbon Dioxide," International Journal of Heat and Mass Transfer, Vol. 10, 1967, pp. 1499-1508.
6 Simoneau, R. J., Williams, J. C., III, and Graham, R. W., "Velocity and Temperature Profiles in Near-Critical Nitrogen," ASME Paper No. 71-HT-23.
7 Bourke, P. J. and Pulling, D. J., "Experimental Explanation of Deterioration in Heat Transfer to Supercritical Carbon Dioxide," ASME Paper No. 71-HT-24.
8 Wilson, M. T., Skoglund, V. J., and Rodgers, J. D., "Radial Flow Measurements of Hydrogen Near Its Critical Point in a Heated Cylindrical Tube," ASME Paper No. 71-HT-25.
9 Hendricks, R. C., Baron, A. K., and Peller, I. C., "GASP - A Computer Code for Calculating the Thermodynamic and Transport Properties for Ten Fluids: Parahydrogen, Helium, Neon, Methane, Nitrogen, Carbon Monoxide, Oxygen, Fluorine, Argon, and Carbon Dioxide," NASA Technical Note D-7808, Feb. 1975.
10 Kays, W. M., Convective and Mass Transfer, McGraw-Hill, New York, 1966.
11 Eckert, E.R.G. and Drake, R. M., Heat and Mass Transfer, McGraw-Hill, New York, 1959.

TABLE I. - HEAT TRANSFER COEFFICIENTS

Flow geometry	P_∞, MPa	T_∞, K	T_w, K	U_∞, m/sec	q, W/cm^2	Pr	Re_x x10^{-6}	h_{exp}, W/cm^2 K	h_{calc}, W/cm^2 K
Vertical	3.767	109.8	122.9	0.642	3.05	1.383	0.996	0.233	0.171
	3.699	110.7	143.5	.655	6.08	1.395	1.032	.185	.174
	3.741	110.1	173.7	.653	9.18	1.·/	1.019	.144	.173
	3.734	110.6	191.3	.670	12.08	..393	1.054	.150	.177
	3.683	110.3	210.0	.659	15.15	1.392	1.033	.152	.175
Horizontal - plate up	3.779	110.1	125.5	.642	3.07	1.386	1.001	.199	.171
	3.817	110.4	145.2	.662	6.08	1.387	1.036	.175	.175
	3.759	110.0	173.3	.641	9.15	1.386	.998	.145	.171
	3.701	110.4	210.1	.655	12.05	1.392	1.028	.121	.174
	3.670	110.6	255.1	.664	15.22	1.395	1.046	.105	.176
Horizontal - plate down	3.684	110.2	124.2	.663	3.07	1.390	1.037	.219	.176
	3.786	110.4	147.0	.665	6.07	1.389	1.041	.166	.176
	3.786	110.3	218.1	.657	9.08	1.387	1.027	.084	.174
	3.803	109.7	a200.1	.670	12.09	1.381	1.037	a.133	.177
	3.748	110.7	a268.9	.697	15.29	1.393	1.097	a.097	.183
Gas - vertical	3.742	272.4	340.9	2.61	3.14	.743	.928	.0458	.0301
Gas - horizontal up	3.745	300.4	394.·	2.75	3.16	.724	.823	.0335	.0291
Gas - horizontal down	3.766	280.5	368.0	2.74	3.13	.737	.931	.0358	.0308

[a]Flow appear locally unstable.

VENT

BACK
PRESSURE
CONTROL

DUMMY LEG

TEST SECTION AND
INSTRUMENT TEE
ASSEMBLY

WARMING

FLOW

VENT

FLOW
CONTROL
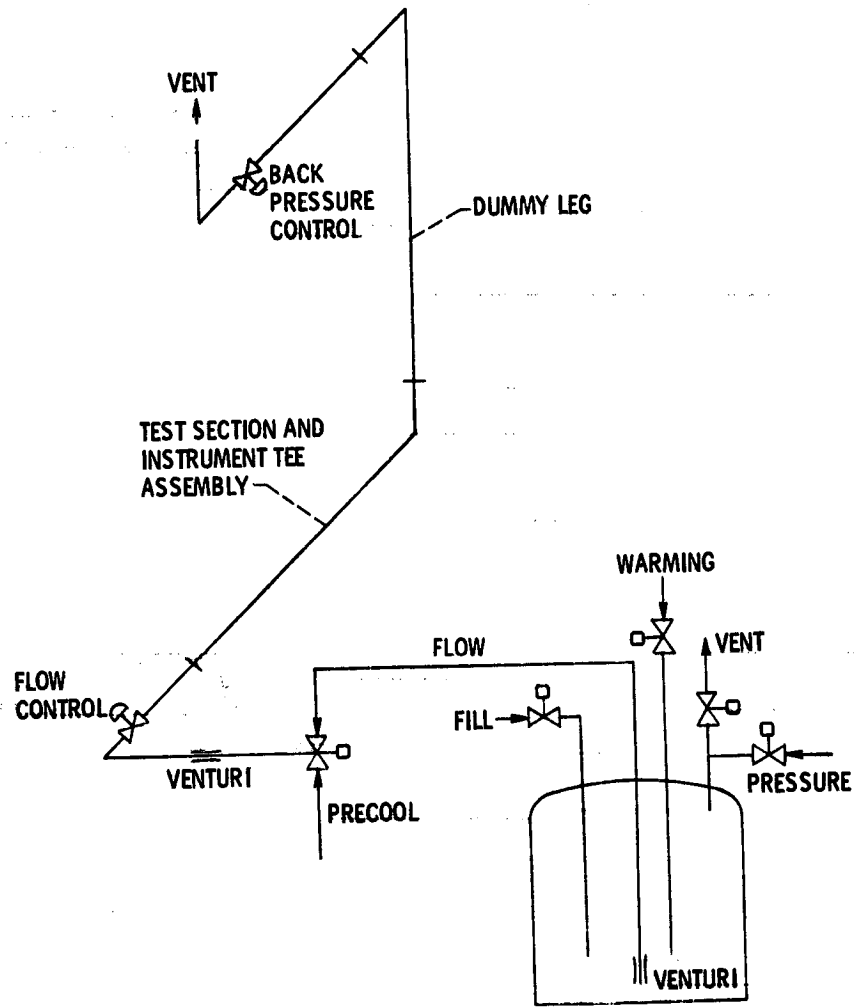
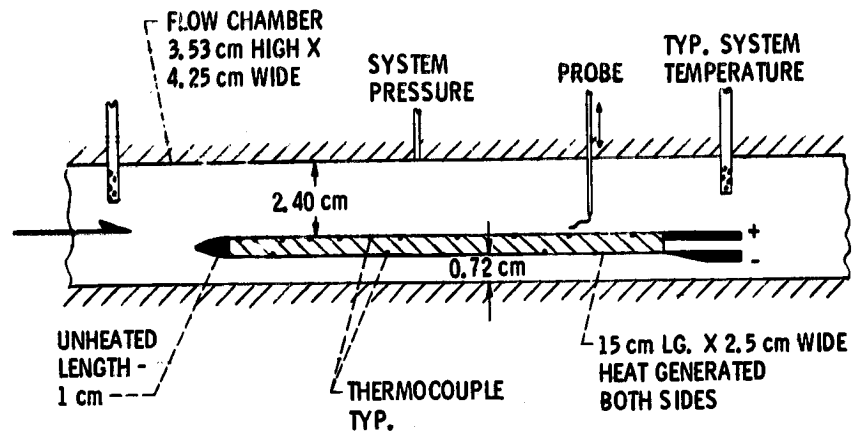FILL

VENTURI

PRECOOL

PRESSURE

VENTURI

Figure 1. - Flow schematic.

Figure 2. - Test section details.
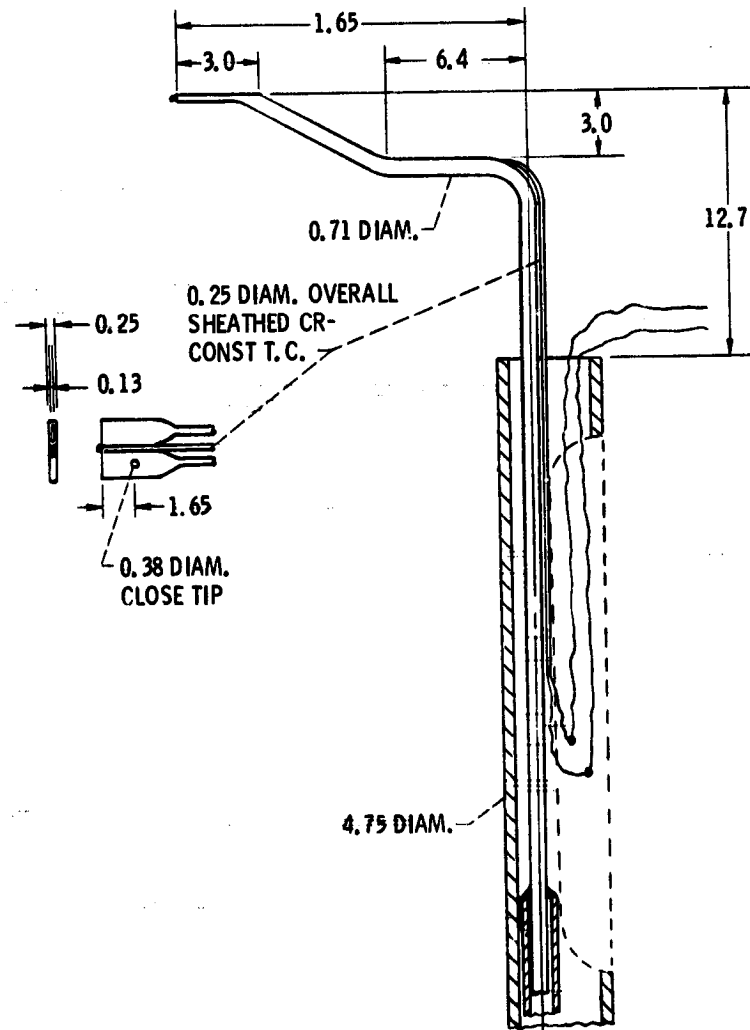

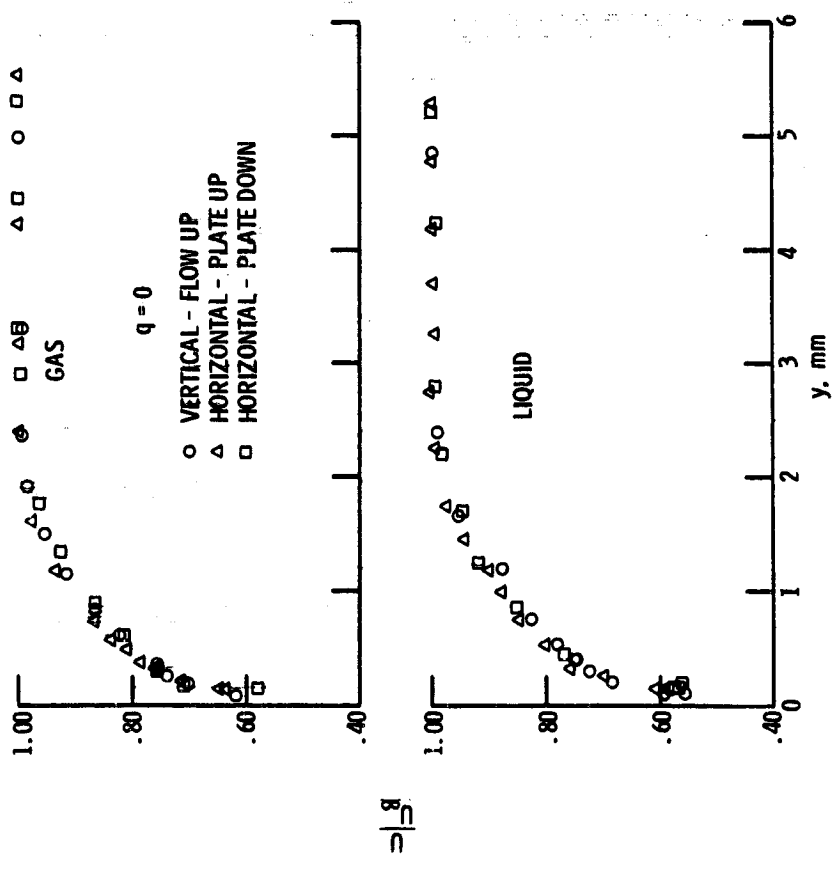Figure 3. - Combination temperature and dynamic pressure probe.
All dimensions in mm.

Figure 5. - Boundary layer flow over heated flat plate in near-critical nitrogen.
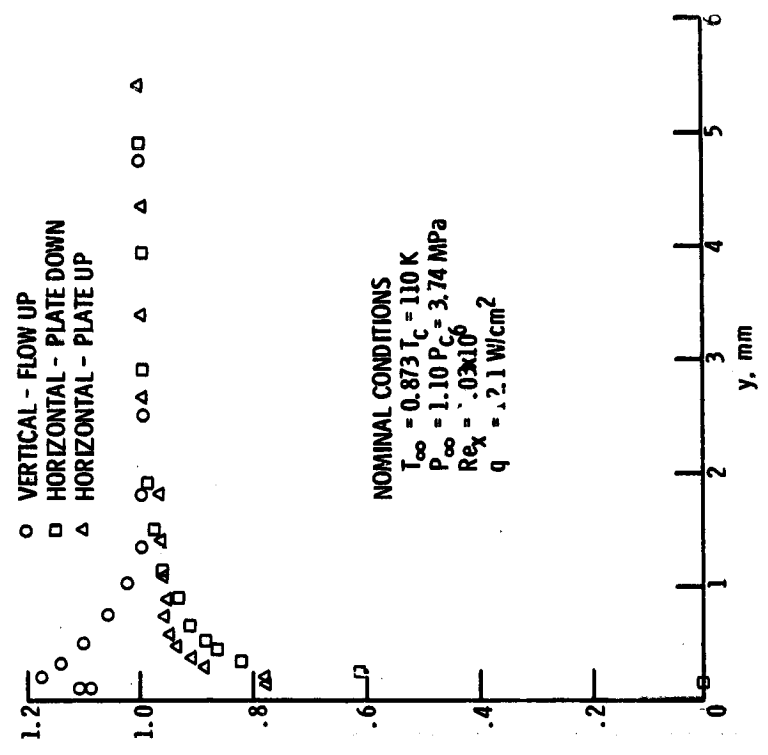
○ VERTICAL - FLOW UP
□ HORIZONTAL - PLATE DOWN
△ HORIZONTAL - PLATE UP

NOMINAL CONDITIONS
$T_\infty = 0.873\, T_c = 110$ K
$P_\infty = 1.10\, P_c = 3.74$ MPa
$Re_x = .03 \times 10^6$
$q = 2.1$ W/cm^2

$\dfrac{u}{u_\infty}$

y, mm

Figure 4. - Velocity profiles for flow past an unheated flat plate.

$q = 0$

GAS

○ VERTICAL - FLOW UP
△ HORIZONTAL - PLATE UP
□ HORIZONTAL - PLATE DOWN

LIQUID

$\dfrac{u}{u_\infty}$

y, mm
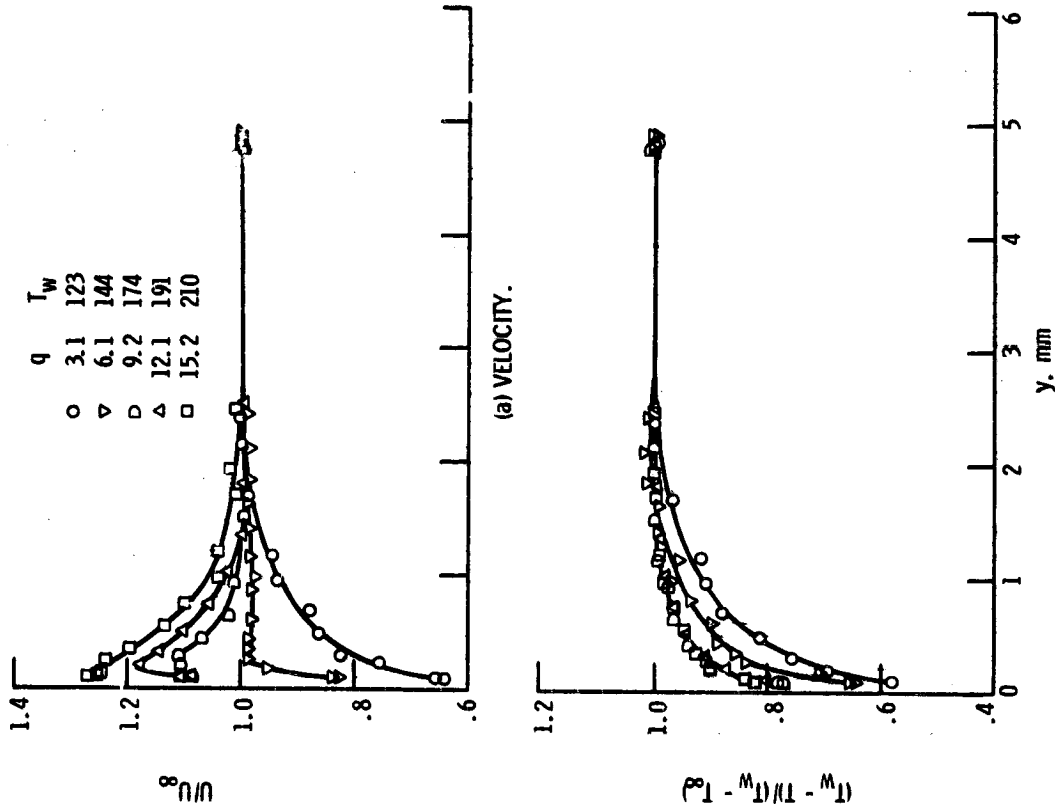
Figure 6. – Boundary layer profiles in vertically upward flow (T_∞/T_c = 0.87; P_∞/P_c = 1.10).
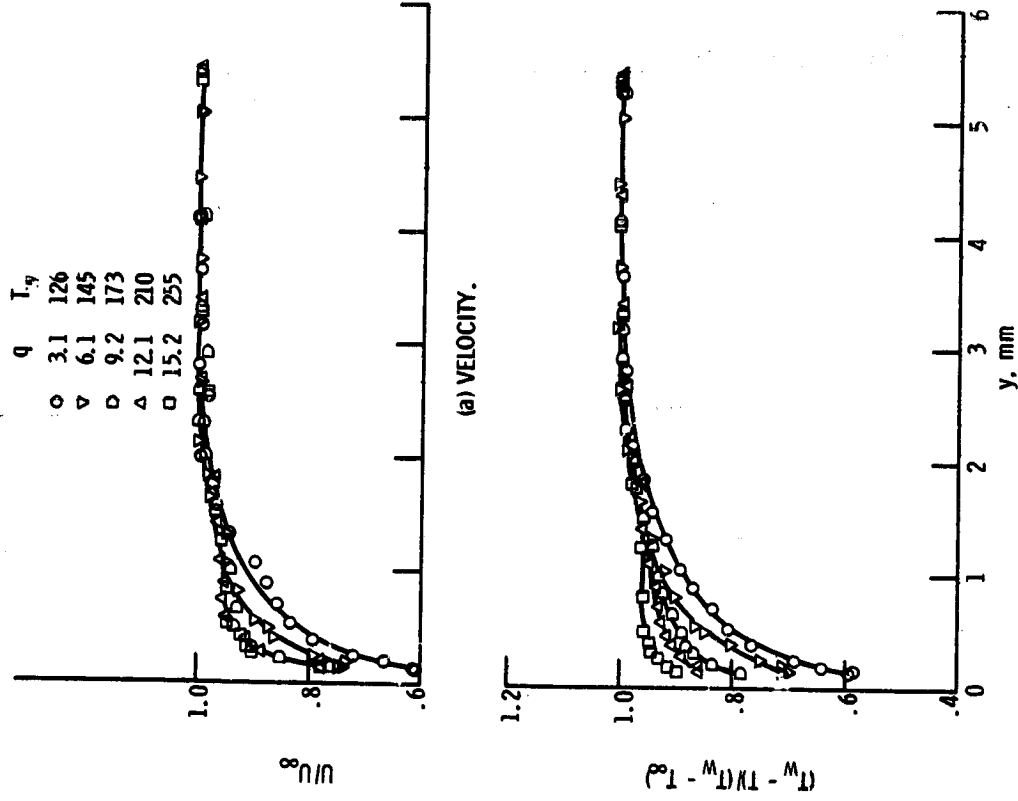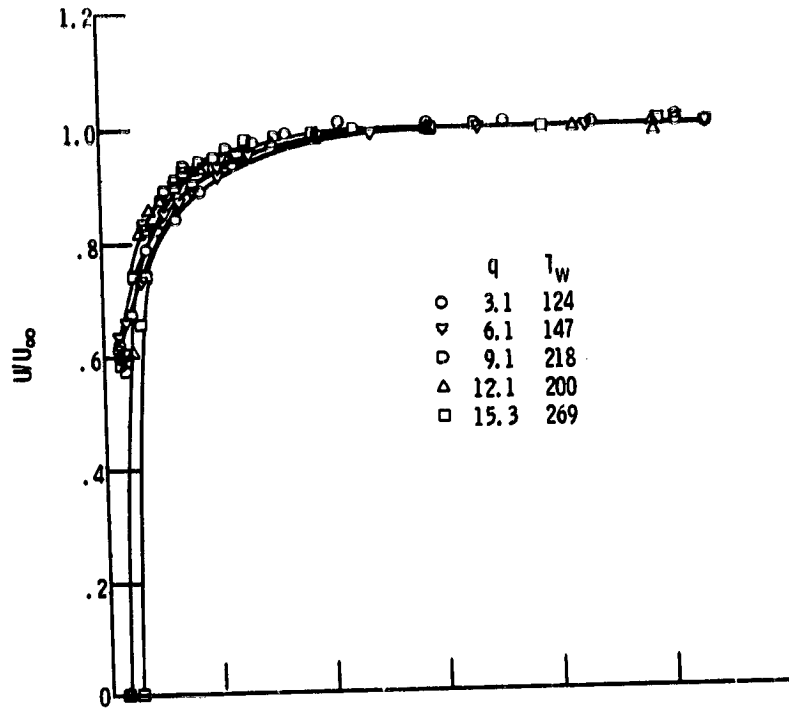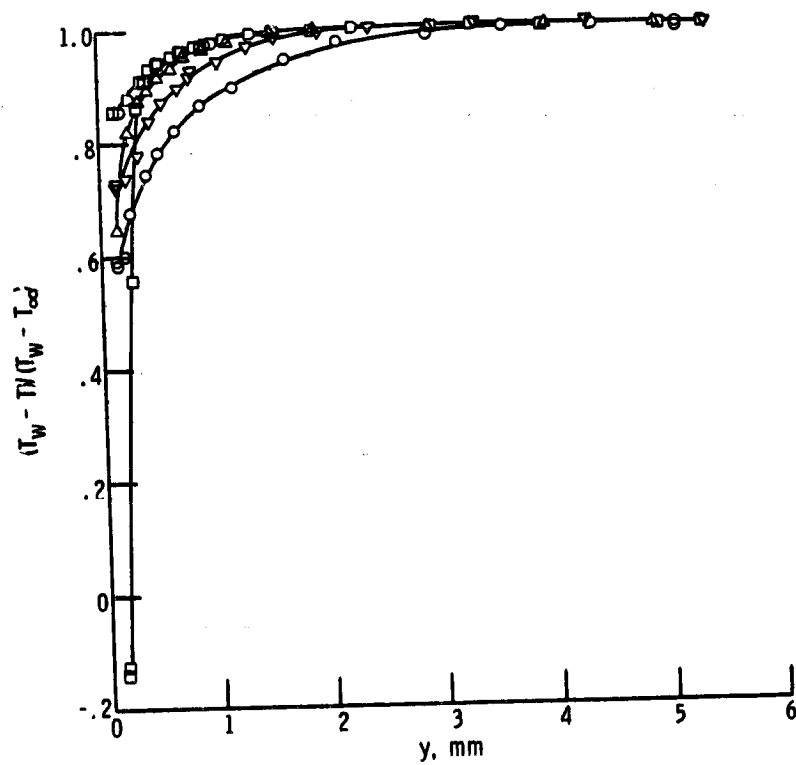
Figure 7. – Boundary layer profiles in horizontal flow with heater facing upward (T_∞/T_c = 0.87; P_∞/P_c = 1.10).

	q	T_w
○	3.1	124
▽	6.1	147
◻	9.1	218
△	12.1	200
◻	15.3	269

(a) VELOCITY.

(b) TEMPERATURE.

Figure 8. – Boundary layer profiles in horizontal flow with heater facing downward (T_∞/T_c = 0.87; P_∞/P_c = 1.10).
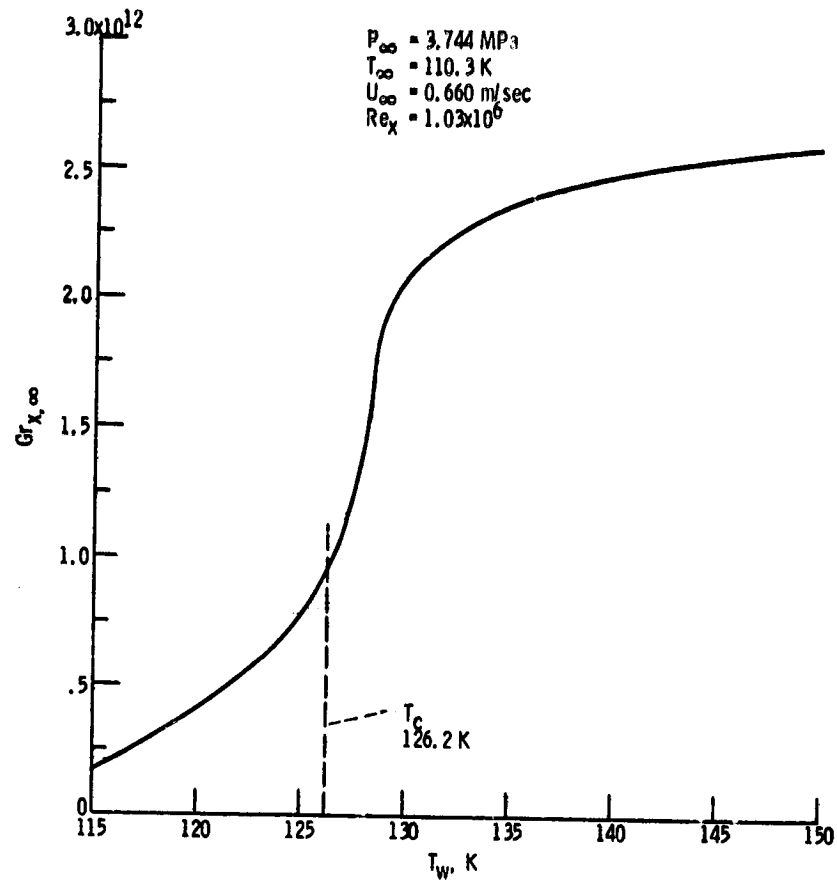
Figure 9. – Variation in Grashof number over the range of the experiment for the nominal operating conditions.